VOL. 20, NO. 2, 2021, 42-48
www.elektrika.utm.my
ISSN 0128-4428

ELEKTRIKA
Journal of Electrical Engineering

FLAUT: A mutual sensitivity improvement through matched pipe, cavity and thin plate resonance

Syamsul Bahrin Abdul Hamid

Kulliyyah of Engineering, International Islamic University Malaysia.

Corresponding author: syamsul_bahrin@iium.edu.my

Abstract: Electrostatic transducers promises a great potential in alternative to piezoelectric transducer based on certain advantages such as inherently wide bandwidth and good acoustic matching to air due to the membrane's low acoustics impedance. There are two basic designs that are popular among electrostatic ultrasonic transducer developer – rigid backplate and micromachine backplate. This paper presents a methodology for improving the sensitivity of an air-coupled ultrasonic transducer by coupling the resonating thin plate, cavity and pipe in a single cell. The proposed device is termed Fluidically Amplified Ultrasonic Transducer (FLAUT) for an air-coupled application. Investigation of the concept of matched thin plate, cavity and pipe, of which the individual geometry is expected to mutually enhance one another. Analytical modelling is utilized to the matched thin plate, cavity and pipe. The analytical modelling identifies the required geometry for the FLAUT based on the matched operating resonant frequency of 25 kHz. At the end of the paper the prototype of FLAUT is presented where the device was fabricated using additive manufacturing process (3-D printing) which consist of a 50 μm Kapton thin film over a micro stereolithography designed backplate. Here aluminum is coated as the electrode utilizing the thermal evaporation process for both the Kapton film and the backplate. A laser interferometer is utilized to measure FLAUT thin plate displacement which indicates the device is running at 25 kHz fundamental mode. A 30 dB difference is also observed between the deformation velocity of the cavity active region and its surrounding.

Keywords: Ultrasonic Amplification, Electrostatic Ultrasonic Transducer, Fluidic Amplification, Capacitive Ultrasonic Transducers

Article History: received 6 April 2021; accepted 26 July 2021; published 28 August 2021.

1. INTRODUCTION

As a promising alternative to piezoelectric transducers especially in the field of non-destructive testing and evaluation (NDE), electrostatic ultrasonic transducers have its own challenges. In general electrostatic transducer offers certain advantage against the conventional piezoelectric transducers such as inherently wide bandwidth [1, 2, 3] and good matching to air due to the membrane's low acoustic impedance [4, 5].

There are two basic designs that are popular among electrostatic ultrasonic transducer developer – rigid backplate and micromachine backplate. With rigid backplate design, there are two main designs: roughened or regularly patterned as shown in Figure 1. According to Hietanen et al [6] and Rafiq and Wykes [7], for a roughened backplate there are few considerations that need to be made - the tension of the membrane, thickness of the membrane, pre-tension of the membrane and the groove geometry. All these parameters will affect the resonance frequency and the performance of the device.

One of key issue highlighted by Pizarro et al [8] and Rafiq and Wykes [7] is the unpredictable nature of the roughened backplate due to air layer variation across the surface of the membrane. Both agreed that the air layer and membrane tension affects the resonant frequency, and causes variation even with the same manufacturing process and setup. This makes it difficult to model the transducer behavior for typical applications since the surface morphology is random. Rafiq and Wykes [7] on the other hand reviewed regular patterned backplate where this type of backplate is found to have a higher sensitivity with two common patterns utilized – v-grooved and cavity. In order to maximize the sensitivity in the v-groove design, and optimization of the groove, angle, grove depth, groove width, membrane thickness and membrane contact is required. Hietanen et al [6], has shown that a shallow groove and a thin membrane such of 8 μm Kapton is able to improve the sensitivity by more than 7 dB and also a fivefold reduction in groove depth could improve the sensitivity by 30 dB. Similar to v-groove design, in cavity design, the sensitivity could be improved by having a light and thin membrane and a shallow cavity design. This however creates an air-stream resistance and squeeze film damping which cause the reduction of sensitivity at higher frequencies. A uniform and well defined pit for cavity design is required to ensure sensitivity of the electrostatic ultrasonic transducers could be maintained [9]. Micromachining process is typically utilized, since the pit geometry and its pit to pit distance variation need to be minimized in order for the electrical and acoustic property of the transducers to be improved [10].

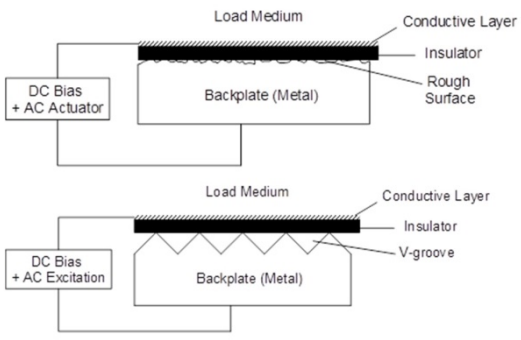

Figure 1. Rigid backplate design, roughened (top) and regularly patterned (bottom)

The Capacitive Micromachine Ultrasonic Transducer (CMUT) by Oralkan et al [11] has the same active component as the generalized electrostatic transducer of membrane and fixed backplate, with CMUT using the semiconductor manufacturing process for fabrication for the membrane and backplate. The CMUT design as in Figure 2 shows the silicone substrate which acts as the bottom electrode with the silicone nitrate acting as the membrane, with the air/vacuum cavity completed sealed.

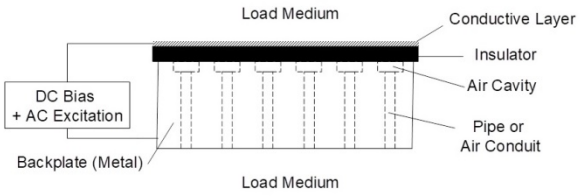

Figure 2. Schematic Diagram of FLAUT with DC biased and AC Excitation Connected

2. CURRENT OPTIMISATION OF ELECTROSTATIC TRANSDUCER

2.1 Bias Voltage

Increasing the bias voltage is a possible way to improve the sensitivity, however in CMUT this would eventually cause the membrane to collapse. Observation by Oralkan et al [11], shows that a collapse-mode CMUT is efficacious in comparison to the conventional CMUT due to the nature of the output pressure and strength of electric field while in collapse-mode. However, for a non-resonant operation, the reduction of the smooth area surface displacement would inherently reduce the sensitivity of the device [8].

2.2 Membrane Configuration

Rafiq and Wykes [7] concluded that sensitivity of the device could be improved by using a thin membrane using the benefit of its flexibility and better contact to backplate surface but is easily damaged [12]. Other membrane configuration membrane configuration has also been proposed such as using a combination of spring type and corrugated membrane [13] and using low stress polysilicone membrane [14], which has shown to improve the sensitivity by -17 dB and -34 dB respectively.

2.3 Air Gap Configuration

Experimentation by Hietenan et al [5] shows that reducing air gap between the membrane and the surface of the backplate has shown improvement on the sensitivity of the device in general. It was observed that a sensitivity of 40 dB is observed when the ridge angle and the groove depth are reduced. However, there is a limit to the improvement that could be achieved. Scheeper et al [1] and Ergun et al [4], observed that thin air gap will increase air stream resistance and the squeeze film damping, which reduces the device sensitivity. This could however be mitigated temporarily through sealing the cavity. This however will cause malfunction of the device if the seal breaks and contaminates the device. Water vapor also reduces the sensitivity of the device or cause the device cease to function [15].

3. PROPOSED DESIGN TO ENHANCED ELECTROSTATIC TRANSDUCER

Considering that ultrasonic transducer is a type of condenser microphone, by taking the design of the condenser microphone it could be observed that an acoustic relief is a way to improve the sensitivity issues of the device. This could be performed by reducing the effect of squeeze film damping and resistance.

This method which is also proposed by Campbell [17] is a concept to improve the sensitivity of electrostatic transducer by employing a resonance of pipe and cavity. The device is governed by few key dimensions: pipe radius and length, cavity radius and depth, and the membrane thickness. The device design is similar to the typical condenser microphone previously discussed, except on the design and construction of the acoustic relief. Further, Zhu et al [18], have validated through experiments that having single cavity and a backplate of 13 individual acoustic relief holes connected to acoustic amplifying pipes have a normalized transmitting voltage response (TVR) of 4.6 times larger than standard device with -6 dB bandwidth. Repeatability of the experiments indicates that the fabrication and measurement are repeatable using the additive manufacturing process.

The proposed design is named FLudically Amplified Ultrasonic Tranducer or FLAUT in short. This design features a backplate with an array of consecutive concentric cavity and pipes as shown in Figure 3. This is contrary to the single cavity and multiple acoustic relief pipes design in condenser microphone as discussed by Tan and Miao [16] and Lavergne et al [19]; which are then adapted by Zhu et al into a single cavity and multiple pipes design [18].

In a conventional electrostatic transducer, the vibrating membrane on top of the cavity will be the only active face coupled to the load medium. However for FLAUT, the AC excited vibrating membrane could also excite the fluid filled pipes, thus amplifying the overall signal. Both gas and liquid were considered as fluid in this case. There are two active faces that are coupled to the load medium – the membrane and the output of the pipes. A perfect acoustic matching between the fluid load media and the pipes output is shown when the pipes are filled with fluid. Since all cavities are coupled directly to the load medium through the concentric pipes, there is no need for a pressure equalization to reduce the effect of squeeze film damping and resistance. Thus the main different between FLAUT and previous papers is the use of concurrent direct one to one coupling between membrane, cavity and pipes.

4. ANALYTICAL MODELLING OF FMUT

This section describes the steps taken to model the FMUT components individually which later will be used for the analytical model for matching purposes.

4.1 Modelling of Thin Plate

In this section, the modelling of the thin plate is explained. It is important to be able to differentiate the difference between a membrane and a thin plate. Previous authors have used the term interchangeable. To clarify the term, Kinsler et al [20], have made a differentiation based on the different restoring force acting upon them - membrane's restoring force is entirely due to tension applied, whilst the plate restoring force is entirely due to the stiffness of the diaphragm.

Ventsel and Krauthammer [21] in their work has defined the thick and thin plate, and membrane based on the ratio of plate diameter against the thickness of the plate. As a guide, a thick plate is when the ratio is less than 10, a membrane is when the ratio is more than 80, and anything in between is thin plate. This could be clearly seen from the (1). As the diaphragm thickness, d_m reduces to a negligible value; the flexural rigidity of diaphragm becomes zero as denoted by Equation (1). This concept illustrates the transitional changes from thin plate to a membrane.

$$D = \frac{E d_m^3}{2(10v^2)} \quad (1)$$

where E is the Young's modulus, v is the Poisson's ratio, d_m is diaphragm thickness.

The diaphragm design was based on the assumption that it was a thin plate, thus no tension is considered. This was referring to the work of Kinsler et al [20] and Rafiq and Wykes [7] which has shown that the resonance frequency of the capacitive transducer depended only on the thickness of the diaphragm and the geometry of the backplate. This has also been corroborated by Hietenen et al [6], which has demonstrates that the effect of tension to the resonance frequency could be neglected for electrostatic transducer.

Modelling of cavity in FLAUT was considered by assuming that a thin plate suspended over a cavity can be approximated by a simple mass-spring system. Assuming piston resonator surrounded by an infinite baffle [20], the resonant frequency of such a mass-spring system can be calculated from Equation (2).

$$f_n = \frac{1}{2\pi}\sqrt{\frac{k}{m}} \quad (2)$$

where k is the total stiffness of the system and m is the supported mass.

In this case, the resonant frequency for a circular thin plate fixed at the edges can be written,

$$f_n = \frac{K_n}{2\pi}\sqrt{\frac{Dg}{w r_m^4}} \quad (3)$$

where K_n is a constant and take the numerical value 10.22 for circular thin plate fixed at the edges operating in the fundamental mode, D is the flexural rigidity of the thin plate and is defined by Equation (1) - with d_m representing the thin plate thickness, r_m is the radius of the thin plate, g is the gravitational acceleration = 9.81 $m{\cdot}s^{-2}$, w is the force or load due to the mass of the thin plate per unit area, which is given by $w = mg/A = \rho_m d_m g$, where ρ_m is the density of the thin plate. Substituting this equation into Equation (3) gives Equation (4), which is the resonant frequency of the thin plate,

$$f_n = \frac{1}{2\pi}\sqrt{\frac{K_n^2 D}{\rho_m d_m r_{m.}^4}} \quad (4)$$

4.2 Modelling of Cavity

The modelling of the cavity takes into assumption that the air follows adiabatic compression laws and where the first law of thermodynamics is used to show the stiffness of the air gap [22], as in Equation (5),

$$k_a = \frac{\gamma P A}{d_a} \quad (5)$$

where the adiabatic constant of air, γ = 1.4, P = 101.325 kPa is the atmospheric pressure and d_a is the thickness of the cavity. Substituting Equation (5) into Equation (2), gives the resonant frequency due to the air cavity as in Equation (6).

$$f_n = \frac{1}{2\pi}\sqrt{\frac{\gamma P}{\rho_m d_m d_a}} \quad (6)$$

From Equation (3) and Equation (6), it could be summarized that the two main resonant frequencies of the FLAUT could be determined, which are the thin plate resonant frequency and the cavity resonant frequency respectively. These two resonant frequencies, along with the pipe resonant frequency will play a pivotal role in the preliminary design requirement of the FLAUT.

4.3 Modelling of Pipes

This step, along with the previous step will enable thin plate, cavity and pipe resonant frequencies to be matched as the first step in the FLAUT design process. Extensive work has been presented on the physics behind resonant frequencies of pipes [23]. In general, the resonant frequency of a pipe is related to the length of the pipe, the shape of its cross section, i.e. circular, square, elliptical etc., and whether it has closed or open ends.

For a rigid cylindrical pipe, the term open cylinder usually refers to when both of the pipe end are left open; while the term closed usually refers to when one of the pipe end is closed with a rigid surface. In FLAUT, we considered both ends of the pipe to be open; one end is open to the load, while another end is open to the cavity, since there is no rigid surface on the cavity end.

For a pipe that is open at both faces, the wavelength of an acoustic wave propagating along the pipe is determined by Equation (7),

$$\lambda_{\boldsymbol{n}} = \frac{2L_e}{n} \quad (7)$$

where λ is the wavelength, n is the mode of operation and Le is the effective length of the pipe.

Since, the velocity of sound could be represented by the product of wavelength and frequency, the resonant frequency of the open cylindrical pipe can then be substituted and rearranged into Equation (8).

$$f_{\boldsymbol{n}} = \frac{nc}{2L_e} \quad (8)$$

where c is the velocity of sound in the medium, n = 1 for the fundamental harmonics for an open cylindrical pipe and L_e is the length of the standing wave. In practice, L_e is slightly longer than the physical length of the pipe. The extension is known as the pipe end-correction. Extensive experimental work [20] and theoretical work [24] has been performed to identify this end correction.

Kinsler et al [20], Anderson et al [24] proposed the following relationship to account for the end correction based on the Equation 9 below:

$$L_e = L_a + 0.6 r_p \quad (9)$$

4.4 Matching thin plate, cavity and pipe

The main output from the analytical modelling is to determine the fundamental frequency or mode (0,1) of individual thin plate, cavity and pipe resonances. These three resonant frequencies are important, as they will determine the total resultant output of the FLAUT

The ideal scenario would be a perfectly matched thin plate, cavity and pipe resonant frequency of which all the individual component will be displacing in phase thus creating a constructive interference. For this to take place, a matching geometry between the three individual components is required.

In order to exemplify the process consider the following design scenario for a FLAUT transducer with a resonant frequency of between 5 kHz and 100 kHz, using 50 μm thickness Kapton film [25]. The analytical model embodied in Equation (4) and Equation (6) is employed to perform a parameter sweep, Figure 4 details the results. From Figure 4, the suitable resonant frequency and its matching thin plate radius and cavity depth could be identified. In the example above, assuming that a 25 kHz transducer is to be constructed for laboratory validation purpose, then the suggested dimensions is 1151 μm for the thin plate radius and 81 μm for the cavity depth. Since thin plate radius is the cavity radius assuming that the edges of the cavity are clamped, all the required dimensions to build a cavity only design have been identified.

However, since the configuration is designed based on individual geometrical components of thin plate, cavity and pipe, no specific transition definition could be identified to differentiate a shallow cavity to pipe (deep cavity) or from pipe to cavity (short pipe). This is due to fact that the equation of cavity and pipe are bounded by their respective relationship that

relates to the operating resonant frequency as have been shown previously.

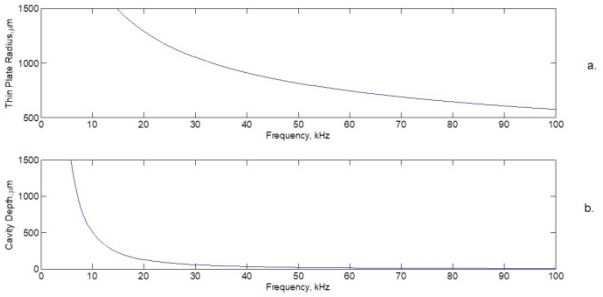

Figure 4. Plot of Parameter Sweep with 50 μm Thickness Kapton for: a. Thin Plate Radius as Function of Frequency and b. Cavity Depth as a Function of Frequency

Next is to identify the matching pipe dimensions. As discussed previously, the pipe radius needs to be as large as practically possible to reduce the squeeze film effect and the air gap resistance. Considering manufacturing constraint, there is a need to ensure that there is a distinct difference in geometry between the cavity diameter and the pipe diameter when the parts are manufactured later. In this case, considering the manufacturing constraint, a 10% reduction from the cavity radius of 1151 μm is selected, giving the pipe radius to be at 1036 μm. At 10% level, the edge-to-edge distance between the radius of the cavity and the radius of the pipe is 115 μm. Pipe length could be identified by re-arranging Equation (10) into Equation (11).

$$L_a = \frac{nc}{2f_n} - 0.6r_p \tag{10}$$

where n = 1 for the fundamental harmonics for an open cylindrical pipe, c is the speed of sound in air at 20°C which is 343 $m{\cdot}s^{-1}$, f_n is the fundamental frequency which is 25 kHz and r_p is the radius of the pipe which is at 1036 μm.

Substituting the above value, results in L_a = 6278 μm. With this, all the required dimensions for a pipe only and a matching thin plate, cavity and pipe design have been identified.

Although from the design stand point, the resonant frequency of all the FLAUT components: thin plate, cavity and pipe are now matched at 2 decimal places accuracy as shown in Table 1; it is important that the tolerances are still maintained during prototyping and manufacturing. Changes in any of the dimensions will change the individual component resonant frequency; thus reducing the effectiveness of the FLAUT amplification.

Table 1: FLAUT Design Dimensions and the Expected Resonance Frequency

Design Parameters	**Plate Resonance, kHz**	**Cavity Resonance, kHz**	**Pipe Resonance, kHz**
Membrane thickness = 50 μm Plate radius = 1151 μm Cavity depth = 81 μm Pipe Radius = 1036 μm Pipe Length = 6278 μm	25 kHz	25 kHz	25 kHz

The output above illustrates the main concept in designing the FLAUT; consideration towards possibility manufacture would need to be considered. As such, with the design parameter above, assuming that the resolution afforded by manufacturing is only at 10 μm, then the resonant of the individual geometry is at 25.03 kHz, 25.15 kHz and 25.00 kHz for thin plate, cavity and pipe resonant frequency respectively. With the 0.6% difference in resonant frequency of the three components, the FLAUT device should still operate within the expected given tolerance.

5. PROTOTYPING OF FMUT

In this section the verification of the modelled FLAUT is discussed, where the two parts of FLAUT, the thin plate and the backplate is prototyped. For the thin plate, Kapton film of thickness 50 μm is used. The plate is then bonded to a metallic ring 56 mm in diameter as shown in Figure 5 (left) where the ring forms part of the transducer assembly. From here when tested, it was also observed that when the pre-tension is minimized, the device reliability is improved, this results matched as per a comments by Schindel et al [9].

The cylindrical backplate with a diameter of 30 mm is then prototyped using additive manufacturing process, a Micro Stereo Lithography (MSL) using 3D printer Objet model Eden 350 [26]. The 3D printer has a net build volume size of 340 mm x 340 mm x 200 mm, with voxel size of 42 μm x 84 μm x 16 μm. The total thickness of the backplate is dependent upon the cavity depth and the pipe length. Finally, aluminum is coated as the electrode utilizing the thermal evaporation process, Edward Coating System model E306A. Typically, the aluminum electrode will have a thickness of 150 nm. Backplate produced using MSL Technique on a Final assembly without membrane is shown in Figure 5 (right).

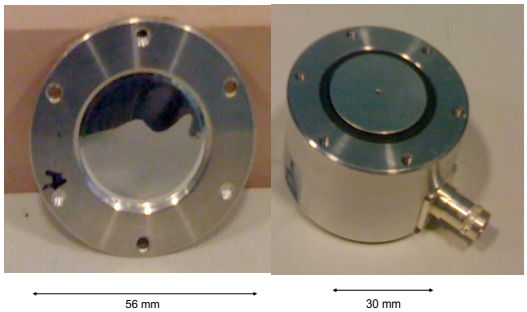

Figure 5. Picture of Kapton Film Bonded on a Metallic Ring (Left) and Backplate Produced using MSL Technique on a Final Assembly Without Membrane (Right)

A full assembly of the device inclusive of the membrane could be seen in Figure 6. From Figure 6, it could be observed that the thin plate has been assembled on top of the slightly protruding MSL backplate with a minimal tension to ensure that no large air bubbles are trapped between the backplate and the membrane.

Figure 6. Picture of Full FLAUT Transducer Assembly

6. RESULTS AND DISCUSSION

In order to corroborate the analytical model, experimental measurements using laser interferometers have been conducted using the manufactured FLAUT prototype.

6.1 Comparison and recognition

There are three different measurement types that could be performed using the laser interferometer based system which are displacement, velocity or acceleration. In addition to the different measurement types, different measurement locations or techniques could be performed using the laser interferometer based system such as a single point measurement, a cross section measurement, and an average surface displacement/velocity/acceleration measurement.

Although it is possible to perform a single point measurement using the laser interferometer based system, it is not possible to accurately pin point the exact center of the thin plate. Thus, it is more appropriate to perform a total surface displacement scan. The surface deformation data from a 25 kHz FLAUT device are shown in in three different views through Figure 7, Figure 8 and Figure 9. The measurements were performed with the transducer front face having a distance of 250 mm from the laser interferometer mirror face. Five points, in a cross formation, distributed equally across the transducer surface have been utilized to align the laser. In terms of corroboration, these laser measurement data are able to indicate the mode shape observed during measurements. For example, in all the previous figures the mode shape that the laser has visualized is the fundamental mode (0, 1). Utilizing the 3 different views, it could be clearly observed that in 3D, the fundamental mode is represented by the semi hemisphere domed shape as shown in Figure 7.

Next, in 2D plan view, with two different views - the magnitude and phase; the mode shape could be observed through visualization with color spectrum moving from green to red representing magnitude of the velocity from low to high. The phase on the other hand, indicates the level of phase uniformity within the surface displacement with relevant phase value utilizing the same spectral concept.

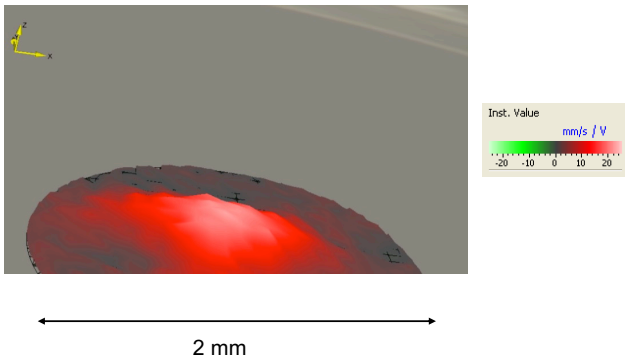

Figure 7. Plot of 3D View of Thin Plate Surface Deformation

From the magnitude plot in Figure 8 (left), it could be observed that the circular center has a higher magnitude compared to the circumference which also indicate a mode (0,1) in plan view – with 3D equivalent of which the center of the dome having a higher amplitude compared to its edges. The phase plot in Figure 8 (right) also indicates that almost all surfaces are in phase. Lastly, in the 2D cross section, a further quantization of the level of deflection across the surface of the membrane could be made. As in the previous 2D plan visualization, in 2D cross section visualization, the magnitude across the section of the plan is made, with the magnitude of the cross section visualized shown in Figure 9.

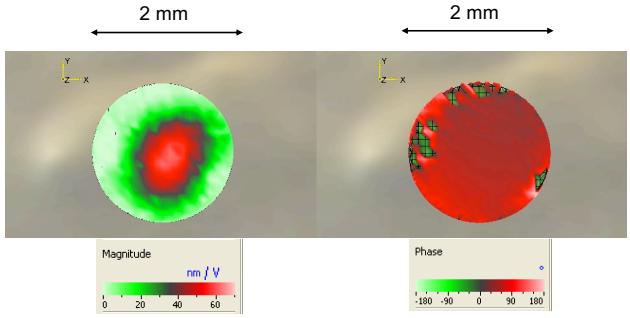

Figure 8. Plot of a 2D Plan View of Thin Plate Surface Displacement: Magnitude (Left) and Phase (Right)

From the measurement, it could be observed that the mode shape is mode (0, 1) fundamental with a dome shaped peak at the center of the membrane is observed as expected by the analytical model. These three visualization and corroboration techniques are important to enable the visualized measured mode shape to be corroborated with the expected mode shape effectively.

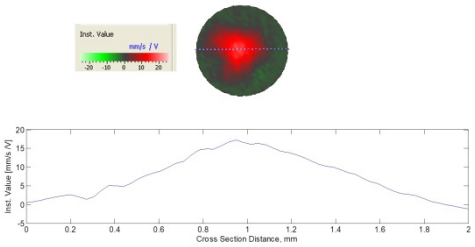

Figure 9. Plot of Cross Section View of Thin Plate Surface Velocity

It should be noted that the visualizations observed by the user through the laser interferometer based system still depends on the excitation frequency and voltage specified to the transducer. There are three types of excitations that could be applied to the transducer, a continuous sinusoidal wave at a desired frequency (narrow band), a single cycle sinusoidal frequency excitation or an impulse excitation (wide band) and a sinusoidal frequency sweep (periodic chirp). The choice of excitation will depend on the FLAUT prototype being measured. In most cases, the periodic chirp excitation signal as shown in Figure 10 is utilized to identify the measured frequency response of a thin plate displacement for a FLAUT device due to its higher frequency content when compared to the single cycle excitation. A frequency domain response of thin plate displacement for a FLAUT transducer designed at 25 kHz is shown in Figure 11. From Figure 11, it could be observed that there are various peaks within the plot. However, as observed, the highest peak is at 25 kHz, which is the fundamental mode of the device.

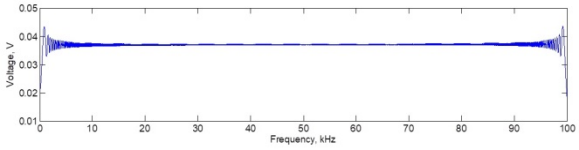

Figure 10. Plot of Periodic Chirp Excitation in Voltage as a Function of Frequency

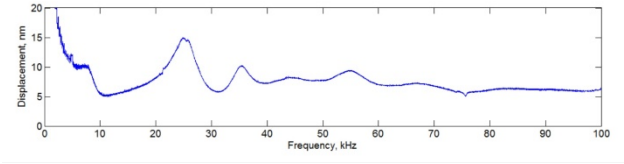

Figure 11. Plot of FLAUT Thin Plate Average Displacement as a Function of Frequency

Previously, in Figure 9, the cross section of membrane surface deformation across the cavity diameter has been plotted. However, the plot only illustrates that the FLAUT is behaving in the fundamental mode (0,1) with the maximum amplitude at the center of the cavity. Although, the plot in Figure 9 shows that the velocity at the circumference of the cavity is low at around ±0.5 mm·s^{-1}/V and thus the circumference could be considered clamped by the bias voltage; there is still a possibility that the rest of the surface is vibrating at a higher velocity. As such, full surface deformation scans for the backplate with the diameter of 30 mm have been performed at 25 kHz as shown in Figure 12.

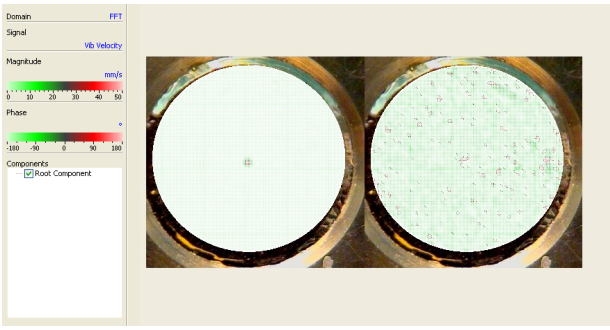

Figure 12. Plot of a 2D Plan View of Thin Plate Surface Velocity for the 30 mm Diameter Electrostatic Transducer Backplate: Magnitude (Left) and Phase (Right)

From the magnitude plot in Figure 12 (left), it could be observed that there is a higher surface deformation across the surface of the cavity compared to the rest of the backplate. This could observe when comparing the center of the backplate with higher velocity in red compared to the rest in the green. This does indicate that the bias voltage is clamping the surface sufficiently as expected. Investigation on the phase of Figure 12 (right) reveals that there is a small random anti-phase area across the surface, suspected due to the air trapped underneath.

When a further cross section of the plot is performed, the different level of deformation across the surface of the thin plate could be clearly seen as shown in Figure 13. From the plot in Figure 13, it could observed that at the center of the cavity, deformation velocity is at 41.4 mm·s^{-1}/V, while at the surface area away from the cavity have the deformation velocity of 1.3 mm·s^{-1}/V; a 30 dB difference. Thus, as the different is significant, it could be proposed that the electrostatic clamping afforded by the bias voltage is sufficient. In addition, as observed in Figure 13, the measured distance between the peripheral edges of the cavity from the surface deformation measurement is almost the same as the cavity diameter. With this respect, the assumption that the thin plate is clamped at the circumference is corroborated.

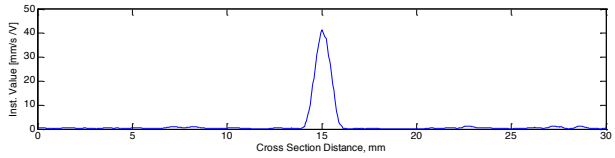

Figure 13. Plot of Cross Section View of Thin Plate Surface Velocity, mm·s-1/V for 30 mm Diameter Electrostatic Transducer Backplate

Although it shows that the velocity outside the cavity is almost flat in comparison to the velocity of the cavity center, there is still a possibility of a surface wave propagating from the center of the cavity due to the thin plate displacement to the edges of the 30 mm backplate and further to the 32 mm metallic ring. Therefore an extended view for the Thin Plate cross section outside the cavity for different phases has been plotted as shown in Figure 14. From here two possibilities could be considered – vibration due to air pockets and the surface wave propagating from the center of the cavity.

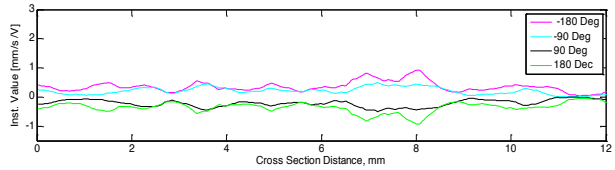

Figure 14. Plot of Thin Plate Surface Deformation Outside the Cavity Periphery for Different Phases

6. CONCLUSION

This paper has presented a backplate design connecting conventional cavity to an open pipe. The design utilizes a matched resonant frequency of thin plate, cavity and pipe to enhance the overall sensitivity of the device. The frequency of individual FLAUT components can be carefully controlled through specific parameters in the backplate. The principles were studied using mathematical analytical equations to identify suitable thin plate thickness and individual cavity and pipe geometry. A suitable geometry that matched a resonant frequency of 25 kHz for cavity and pipe, and suitable thin plate thickness were selected for prototyping. The FLAUT backplate is manufactured using an additive manufacturing technique and then aluminum coated utilizing the thermal evaporation process. Measurements were performed using laser interferometer Polytec PSV300 Scanning Laser Vibrometry System. A frequency domain response with periodic chirp excitation indicates that the thin plate displacement for a FLAUT designed at 25 kHz have multiple peaks. However, it is observed that the highest peak of 15 nm displacement is at 25 kHz and have a fundamental mode shape (0,1).

REFERENCES

[1] P. Scheeper, A. G. H. van der Donk, W. Olthuis and P. Bergveld, "A Review of Silicone Microphones," *Sensors and Actuators,* vol. 44, pp. 1-11, 1994.

[2] NDT Education Resource Centre, "Wave Propagation," NDT Education Resource Centre;, 2012. [Online]. [Accessed 2018].

[3] NDT Education Resource Centre, "Mode Conversion," NDT Education Resource Centre, 2014. [Online]. [Accessed 2018].

[4] A. S. Ergun, B. Temelkuran, E. Ozbay and A. Atalar, "A New Detection Method for Capacitive Micromachine Ultrasonic Transducers," *IEEE Transactions on Ultrasonics, Ferroelectrics, and Frequency Control,* vol. 48, pp. 932-942, 2001.

[5] J. Hietanen, P. Mattila, J. Stor-Pellinen, F. Tsuzuki, H. Väätäjä, K. Sasaki and M. Luukkala, "Factors Affecting the Sensitivity of Electrostatic Ultrasonic Transducers," *Measurement Science and Technology,* vol. 4, pp. 1138-1142, 1993.

[6] J. Hietanen, J. Stor-Pellinen, M. Luukkala, P. Mattila, F. Tsuzuki and K. Sasaki, "A Helmholtz Resonator Model for an Electrostatic Ultrasonic Air Transducer with a V-grooved Backplate," *Sensors and Actuators,* vol. 39, pp. 129-132, 1993.

[7] M. Rafiq and C. Wykes, "The Performance of Capacitive Ultrasonic Tranducer Using V-Grooved Backplate," *Measurement Science and Technology,* vol. 2, pp. 168-174, 1991.

[8] L. Pizarro, D. Certon, M. Lethiecq and B. Hosten, "Airborne Ultrasonic Electrostatic Transducers With Conductive Grooved Backplates: Tailoring Their Centre Frequency, Sensitivity And Bandwidth," *Ultrasonics,* vol. 37, pp. 493-503, 1999.

[9] D. W. Schindel, A. Hutchins, L. Zou and M. Sayer, "The Design and Characterization of Micromachined Air-Coupled Capacitance Transducer," *IEEE Transactions on Ultrasonics, Ferroelectrics and Frequency Control,* vol. 42, pp. 42-50, 1995.

[10] S. G. McSweeney and W. M. D. Wright, "HfO2 High-k dielectric Layers in Air-coupled Capacitive Ultrasonic Transducers," *IEEE International Ultrasonic Symposium,* pp. 864-867, 2011.

[11] Ö. Oralkan, B. Bayram, G. G. Yaralioglu, A. S. Ergun, M. Kupnik, D. T. Yeh, I. O. Wygant and B. T. Khuri-Yakub, "Experimental Characterization of Collapse-Mode CMUT Operation," *IEEE Transactions on Ultrasonics, Ferroelectrics, and Frequency Control,* vol. 53, pp. 1513-1523, 2006.

[12] E. Campbell, L. A. J. Davis, G. Hayward and D. Hutchins, "Cross-Coupling in Sealed cMUT Arrays for Immersion Applications.," in *2007 IEEE Ultrasonics Symposium Proceedings*, 2007 IEEE Ultrasonics Symposium Proceedings New York City, NY, USA, 2007.

[13] M. Füldner, A. Dehé and R. Lerch, "Analytical Analysis and Finite Element Simulation of Advanced Membranes for Silicone Micrphones," *IEEE Sensors Journal,* vol. 5, pp. 857-863, 2005.

[14] P. C. Hsu, C. H. Mastrangelo and K. D. Wise, "A High Sensitivity Polysilicon Diaphragm Condenser Microphone," in *IEEE Eleventh Annual International Workshop on Micro Electro Mechanical Systems*, Heidelberg, Germany, 1998.

[15] S. T. Hansen, A. S. Ergun, W. Liou, B. A. Auld and B. T. Khuri-Yakub, "WIdeband Micromachines Capacitive Microphone with Radio Frequency Detection," *Acoustical Society of America,* vol. 2004, pp. 828-842, 116.

[16] C. W. Tan and J. Miao, "Design Optimization of Condenser Microphone: A Design of Experiment Perspective," *Journal Acoustic Society of America,* vol. 125, pp. 3641-3646, 2009.

[17] E. Campbell, W. Galbraith and G. Hayward, "A New Electrostatic Tranducer Incorporating Fluidic Amplification," in *2006 IEEE Ultrasonics Symposium*, Vancouver, BC, Canada, 2006.

[18] B. Zhu, B. P. Tiller, A. J. Walker, A. J. Mulholland and J. F. C. Windmill, "“Pipe Organ” Inspired Air-Coupled Ultrasonic Transducers With Broader Bandwidth," *IEEE Transactions on Ultrasonics, Ferroelectrics, and Frequency Control,* vol. 65, no. 10, pp. 1873-1881, 2018.

[19] T. Lavergne, S. Durand, M. Bruneau and N. Jol, "Displacement Field of the Membrane of Condenser Microphones at High Frequencie," in *Acoustics 2012*, Nantes, France, 2012.

[20] L. E. Kinsler, A. R. Frey, A. B. Coppens and J. V. Sanders, Fundamental pf Acoustics, John Wiley & Sons Inc., 1982.

[21] E. Krauthammer and T. Ventsel, Thin Plates and Shells: Theory, Analysis and Applications, New York, US: Marcel Dekker Inc., 2001.

[22] T. D. Rossing and N. H. Fletcher, Principles of Vibration and Sound, New York, US: Springer-Verlag, 1994.

[23] A. Wood and J. M. Bowsher, Alexander's Wood's The Physics of Music, London, UK: John Wiley & Sons Ltd, 1975.

[24] S. H. Anderson and F. C. Ostensen, "Effect of Frequency on The End Correction of Pipes," *Physical Review,* vol. 31, pp. 267-274, 1928.

[25] DuPont de Nemours (Luxembourg) s.a.r.l, "DuPont™ Kapton® HN Polyimide Film Technical Data Sheet," 2012. [Online]. [Accessed 2018].

[26] Stratasys Ltd, *Objet Eden 350/350,* Stratasys Ltd, 2013.